

2 **Title: The dengue virus NS1 protein conveys pro-inflammatory**
3 **signals by docking onto human high-density lipoproteins**

4
5 **Authors:** Souheyla Benfrid^{1,2,#,*}, Kyu-Ho Park^{1,#,*}, Mariano Dellarole^{1,#}, James E. Voss^{1,#},
6 Carole Tamietti¹, Gérard Pehau-Arnaudet³, Bertrand Raynal⁴, Sébastien Brûlé⁴, Patrick
7 England⁴, Xiaokang Zhang^{1,#}, Anastassia Mikhailova^{5,#}, Marie-Noëlle Ungeheuer⁶, Stéphane
8 Petres⁷, Scott B. Biering⁸, Eva Harris⁸, Anavaj Sakunthabai⁹, Philippe Buchy^{10,#}, Veasna
9 Duong¹⁰, Philippe Dussart¹⁰, Fasséli Coulibaly¹¹, François Bontems^{1,12}, Félix A. Rey¹, Marie
10 Flamand^{1,†}

11
12 **Affiliations:**

13 ¹Unité de Virologie Structurale, Institut Pasteur and CNRS UMR3569, 25-28 rue du Docteur Roux,
14 75724 Paris, France

15 ²Université Paris Descartes Sorbonne Paris Cité, France

16 ³UTECH UBI, Institut Pasteur and CNRS UMR 3528, 28 rue du Docteur Roux, 75015 Paris, France

17 ⁴Molecular Biophysics Facility, Institut Pasteur, CNRS UMR 3528, 25 rue du Docteur Roux, 75724
18 Paris, France

19 ⁵HIV Inflammation et Persistance, Institut Pasteur, 28 rue du Docteur Roux, 75724 Paris, France

20 ⁶ICAReB, Institut Pasteur, 28 rue du Docteur Roux, 75724 Paris, France

21 ⁷Production and Purification of Recombinant Proteins Facility, Institut Pasteur, 28 rue du Docteur
22 Roux, 75724 Paris, France

23 ⁸Division of Infectious Diseases and Vaccinology, School of Public Health, University of California,
24 Berkeley, Berkeley, CA, USA

25 ⁹Human Genetics, Institut Pasteur, 25 rue du Docteur Roux, 75724 Paris, France

26 ¹⁰Virology Unit, Institut Pasteur du Cambodge, Institut Pasteur International Network, 5 Monivong
27 Boulevard, PO Box 983, Phnom Penh, Cambodia

28 ¹¹Department of Biochemistry and Molecular Biology, Monash University, Clayton, 3800, Australia

29 ¹²Département de Biologie et Chimie Structurales, Institut de Chimie des Substances Naturelles,
30 CNRS UPR2301, Gif-sur-Yvette, France

31 #Present addresses: Université Paris-Est, Laboratoire de Santé Animale, ANSES, INRA, ENVA, UMR
32 1161 Virologie, 94700, Maisons-Alfort, France (SB); Applied Molecular Virology, Institut Pasteur
33 Korea, Seongnam-si, Gyeonggi-do, Rep. of Korea (KHP); Virus Biophysics Laboratory,
34 Bionanosciences Research Center (CIBION), National Scientific and Technical Research Council
35 (CONICET), Godoy Cruz 2390, C1425FQD Ciudad Autónoma de Buenos Aires, Argentina (MD);
36 Department of Immunology and Microbiology, The Scripps Research Institute, La Jolla, CA 92037,
37 USA (JV); Guangdong Provincial Key Laboratory of Brain Connectome and Behavior, CAS Key
38 Laboratory of Brain Connectome and Manipulation, the Brain Cognition and Brain Disease Institute
39 (BCBDI), Shenzhen Institutes of Advanced Technology, Chinese Academy of Sciences; Shenzhen-
40 Hong Kong Institute of Brain Science-Shenzhen Fundamental Research Institutions, Shenzhen,
41 518055, China (XZ); Division of Molecular Neurobiology, Department of Medical Biochemistry and
42 Biophysics, Karolinska Institute, Stockholm, Sweden (AM); GlaxoSmithKline Vaccines R&D,
43 Singapore (PB)

44

45 *These authors contributed equally to this work

46 †Correspondence to: Marie Flamand (marie.flamand@pasteur.fr)

47

48 **ABSTRACT**

49 The nonstructural NS1 protein is a virulence factor secreted by dengue virus (DENV)-infected
50 cells. NS1 is known to alter the complement system, activate immune cells and perturb
51 endothelial barriers. Here we show that pro-inflammatory signals are triggered by a high
52 affinity complex formed between NS1 and human high-density lipoproteins (HDL).
53 Electron microscopy images of the NS1-HDL complexes show spherical HDL particles with
54 rod-shaped NS1 protrusions on their surface. These complexes are readily detectable in the
55 plasma of hospitalized dengue patients using anti-apolipoprotein A-I (ApoA-I) antibodies
56 specific of the HDL moiety. The functional reprogramming of HDL particles by the NS1
57 protein as a means to exacerbate systemic inflammation during DENV infection provides a
58 new paradigm linking the human lipoprotein network to dengue pathogenesis.

59

60

61

62

63 **Short title:** DENV NS1 forms pro-inflammatory complexes with HDL

64

65 INTRODUCTION

66 Dengue virus (DENV) infects nearly 400 million people annually, leading to more than
67 500,000 hospitalizations (1, 2). The mortality rate varies from less than 1% to 10% depending
68 on the epidemic and medical care provided to patients (« Dengue and Severe Dengue » s. d.
69 WHO, 2016, (3)). The dengue nonstructural protein 1 (NS1) is a viral effector circulating in
70 the bloodstream of DENV-infected patients (reviewed in (4-6)). In DENV-infected cells, NS1
71 forms amphipathic dimers in the endoplasmic reticulum (ER) that insert into the luminal side
72 of the membrane (7-9). The membrane-bound dimers play an essential role in orchestrating
73 viral replication in specialized subcellular factories (10). A sub-fraction of NS1 dimers further
74 associate by three to form barrel-shaped hexamers. During this process, NS1 hexamers detach
75 from the ER membrane and are secreted as soluble nanoparticles loaded with lipids from the
76 infected cell (11, 12). The secreted form of NS1 has previously been shown to bind to
77 complement and coagulation factors, to activate immune and endothelial cells, to trigger the
78 expression of pro-inflammatory cytokines, to alter the glycocalyx barrier and to promote
79 endothelium permeability (13-18). The antibody response against NS1 has been shown to
80 protect against several flavivirus infections (14, 19-22) but can also be harmful *via* a cross-
81 reaction with platelets and endothelial cell surface antigens (23-28). These characteristics
82 altogether favor the development of thrombocytopenia, vascular leakage and hemorrhage.
83 Given the growing evidence of NS1 involvement in dengue pathogenesis, a better
84 understanding of the molecular fate of NS1 in extracellular fluids by identifying its interacting
85 partners is of utmost importance.

86
87 In the present study, we report that NS1 from dengue virus serotype 2 (DENV-2) binds high-
88 density lipoproteins (HDL) and with a lower affinity low-density lipoproteins (LDL). HDL
89 and LDL are lipoprotein complexes composed of large lipid cargos enwrapped by the

90 apolipoproteins A-I and B, respectively, as well as a panel of functional proteins recently
91 identified by proteomic approaches (29, 30). Lipoprotein particles that circulate in the blood
92 have long been recognized for their regulatory functions in vascular homeostasis,
93 inflammation and innate immune responses (29, 31-34). We explored the NS1-HDL
94 association by biophysical methods and visualized the complex by electron microscopy. Our
95 observations revealed a stable anchoring of NS1 amphipathic dimers to the HDL surface. We
96 observed that the NS1-HDL complex could trigger the production of pro-inflammatory
97 cytokines in exposed human primary macrophages. In addition, we consistently detected
98 elevated levels of NS1-HDL complexes in the blood of DENV-infected patients on the day
99 of admission to hospital using an anti-apolipoprotein A-I (ApoA-I) detection assay.
100 We further determined that NS1 complexes acquired an apolipoprotein E (ApoE)-positive
101 phenotype during the clinical phase, a component mostly found on very-low-density
102 lipoproteins or chylomicrons and only transiently associated to HDL or LDL. This pointed to
103 a complex and dynamic interaction of NS1 with the host lipoprotein metabolic cycle.

104

105 **RESULTS**

106 **The DENV-2 NS1 hexamer binds high- and low-density lipoprotein particles**

107 In this study, we first sought to identify NS1 protein partners encountered during its
108 circulation in human blood. For this purpose, we carried out a pull-down assay using a
109 purified preparation of recombinant strep-tagged DENV2 NS1 spiked in plasma obtained
110 from healthy donors to pull down potential ligands. We thus re-affinity purified NS1 from the
111 plasma and analyzed the resulting products by size exclusion chromatography (SEC) (Fig.
112 1A). Compared to NS1 alone, the pull-down SEC profile showed an additional peak and a
113 large shoulder at smaller elution volumes, corresponding to apparent molecular weights of

114 840 and 380 kDa, respectively (Fig. 1A). The protein contents of the two high molecular
115 weight complexes were analyzed by SDS-PAGE and the identities of the predominant protein
116 bands determined by N-terminal sequencing and mass spectrometry as ApoA-I and ApoB.
117 These proteins correspond to the main scaffold proteins of HDL and LDL, respectively (Fig.
118 1A).

119 This observation prompted us to assess the affinity of DENV2 NS1 for HDL and LDL.
120 We immobilized human HDL and LDL particles on bio-layer interferometry (BLI) sensors
121 coated with specific polyclonal antibodies against ApoA-I or ApoB, respectively. Figure 1B
122 displays the binding curves for increasing NS1 concentrations in contact with both types of
123 lipoprotein particles, and the values reached at steady state. The curves can be fitted using a
124 single state binding model leading to a relative binding constant (K_d) of $63 \text{ nM} \pm 0.2 \text{ nM}$
125 for HDL and $1.4 \text{ } \mu\text{M} \pm 0.1 \text{ } \mu\text{M}$ for LDL (Fig. 1B), indicating preferential binding of NS1 to
126 HDL compared to LDL.

127 In order to characterize the architecture of the complex, we used analytical ultracentrifugation
128 to study the behavior of NS1, HDL and a mix of NS1 and HDL at either a 1:1 or 5:1 mass
129 ratio, which represents approximately a 0.5:1 or 2.3:1 NS1 hexamer to HDL molar ratio (Fig.
130 1C). Purified NS1 sedimented as a main species with a sedimentation coefficient of 7.9 S
131 compatible with a globular hexamer. HDL particles exhibited a much lower value of 4.20 S
132 in keeping with the larger lipid to protein ratio (35). In the sample containing an excess of
133 NS1 mixed with HDL, all the HDL was engaged in an interaction with NS1 forming a unique
134 species with a sedimentation coefficient of 16.8 S that segregated distinctly from the other
135 species (Fig. 1C). Residual unbound NS1 hexamer could still be observed, as expected due to
136 the NS1 excess (Fig. 1C). By combining two detectors and taking into account the theoretical
137 composition of the HDL particles, we estimated that one NS1 hexamer was bound to each
138 HDL particle when present in excess. Interestingly, in the 1:1 ratio sample, we detected

139 intermediate peaks at 9.4 and 11.7S that corresponded to one or two NS1 dimeric subunits
140 bound to HDL, respectively.

141
142 **Binding of the NS1 hexamer to spherical HDL leads to a surface rearrangement of NS1**
143 **into dimeric rod-shaped protrusions**

144 Based on the above results, we used a 2:1 molar ratio to prepare NS1-HDL complexes and
145 examined the resulting products by negative stain electron microscopy (EM). As previously
146 shown (36), human HDL particles appear as smooth spheres $\simeq 10$ nm in diameter with an
147 electron-dense central region (Fig. 2A). The purified NS1-HDL complexes, in contrast,
148 presented a granular surface with prominent structures on their outer surface (Fig. 2B).
149 2D class averages of NS1-HDL complexes revealed that the HDL particles were crowned
150 with high-density features that match very well the contour of NS1 dimers in side view with
151 two discrete nodules that likely correspond to the NS1 protomers (Fig. 2B, 2C) (7-9). About
152 60% of the complexes analyzed in our study presented three NS1 dimers on the HDL surface,
153 suggesting that NS1 hexamers dissociate into dimers upon binding to HDL particles (Fig. 2B,
154 2C). Around 25% and 10% of the particles presented 2 or 4 apparent NS1 dimers at their
155 surface, respectively. These observations corroborate the ultracentrifugation data showing
156 different ratios of NS1 dimers per HDL particle depending on the initial NS1:HDL ratio (Fig.
157 1C) and suggest a dynamic binding mode between NS1 and HDL particles.

158 The presence of NS1 dimeric subunits associated to HDL was also evidenced by DSC
159 (Fig. 2D). Thermal scanning of both hexameric NS1 and the NS1:HDL mix (at a 2:1 molar
160 ratio) showed two transitions phases while the HDL particles alone did not contribute to any
161 signal in the scanned temperature range (Fig. 2D) (37). The second transition at a T_m of 81°C
162 was identical for NS1 alone and in complex with HDL. We have previously reported that the
163 NS1 dimer of Japanese encephalitis virus requires temperatures higher than 80°C to dissociate

164 into monomers (38). We therefore attributed this second transition to the dissociation and full
165 denaturation of NS1 dimeric subunits (Fig. 2D). Accordingly, the first transition peak
166 corresponds to the dissociation of NS1 hexamers into dimers for NS1 alone (T_m of 59°C) and
167 to the release of NS1 dimers from the HDL particle for the NS1-HDL mix (T_m of 67°C) (Fig.
168 2D). The difference in T_m values observed for the first transition peak in both samples
169 provides additional evidence that once the NS1-HDL complex formed, the NS1 dimer-dimer
170 interface initially present in the hexamer is converted into a more stable interface formed
171 between the NS1 dimers and the HDL surface.

172

173 **The NS1-HDL complex triggers pro-inflammatory signals in human primary**
174 **macrophages**

175 NS1 is known to trigger the production of pro-inflammatory cytokines in macrophages (15).
176 As HDL are potent modulators of inflammation (31, 32), we characterized the cytokine and
177 chemokine production pattern in human macrophages exposed to NS1 alone, HDL alone or
178 to the NS1-HDL complex (Fig. 3B). Primary macrophages were differentiated from isolated
179 monocytes of various donors and stimulated with the different combinations of effectors.
180 When exposed to NS1 or HDL alone, we observed no significant difference in the cytokine
181 levels produced by macrophages compared to the negative control, whereas the bacterial
182 lipopolysaccharide (LPS) consistently induced high levels of cytokine secretion (Fig. 3B).
183 These observations rule out any cytotoxic effect from putative contaminants in the NS1 and
184 HDL samples. In contrast, the NS1-HDL mix induced a significant increase in TNF- α , IL-6
185 and IL-10 secretion, and to a lesser extent IL-1 β , compared to NS1 alone. The differences were
186 even higher when compared with HDL alone, suggesting that NS1 converts HDL into pro-
187 inflammatory signaling particles (Fig. 3B).

189 **NS1-HDL complexes are detected in hospitalized patients**

190 Knowing that the concentration of the above-mentioned cytokines and chemokines is
191 dramatically increased in patients with severe dengue (39-42), we assessed the presence of
192 NS1-HDL complexes in DENV-infected patients. To this end, we developed an additional
193 ELISA format to broadly detect and quantify NS1-lipoprotein complexes in human plasma.
194 In addition to our original NS1 detection assay (43, 44) and to the NS1-HDL semi-quantitative
195 ELISA (Supplementary Fig. 1A,1B), we used an anti-ApoE PAb for the secondary detection
196 of NS1 complexes potentially formed with the various types of lipoprotein particles (VLDL,
197 IDL, chylomicrons in addition to HDL and LDL, as reviewed in (45, 46)) (Supplementary
198 Fig. 1C). Using the three different ELISA formats, we tested blood samples from 51 dengue
199 patients starting on the day of admission to hospital until their discharge. This represented on
200 average a time lag of 4.3 days between the first and last samples. The vast majority of patients
201 (around 80%) showed significantly elevated NS1 and NS1-HDL in blood on the day of
202 admission compared to the last sample (Fig. 3C). The highest levels were observed between
203 day 2 and day 4 post-onset of fever (Fig. 3C). By contrast, concentrations of NS1-ApoE-
204 positive lipoprotein particles increased over time and were highest when tested on the last
205 blood specimen recovered at the time of discharge from hospital (Fig. 3C). At this stage, we
206 do not know whether the NS1-HDL complex recruits the exchangeable ApoE as a maturation
207 or recycling process or whether, once the HDL pool becomes exhausted, the NS1 protein still
208 expressed binds to other types of lipoprotein particles. In any case, our data clearly show a
209 transition in the nature of the complexes formed between NS1 and the host lipoproteins during
210 the course of infection.

211

212 **DISCUSSION**

213 Dengue virus nonstructural protein 1 is a viral virulence factor that contributes to the
214 development of severe dengue, characterized by cytokine storm, thrombocytopenia, vascular
215 leakage and hemorrhage (4-7). NS1 circulates in the blood of infected patients at nanogram
216 to microgram per ml levels (47-49). We previously described that the secreted hexameric
217 form of NS1 shuttles a lipid cargo analogous to those carried by plasma lipoproteins,
218 suggesting a possible interference with the lipoprotein metabolic cycle (12). Herein,
219 we provide evidence of a direct interaction between NS1 and human HDL characterized by
220 the ApoA-I scaffold protein, and with LDL identified by the presence of ApoB. The
221 complexes formed between NS1 and HDL accumulate during the acute phase of the disease
222 and by the end of the hospitalization period, NS1-lipoprotein complexes acquire an ApoE-
223 positive phenotype that may be part of the anti-viral response engaged by the host.

224

225 Once bound to an HDL particle, the NS1 hexamer appears to fuse and collapse into NS1
226 dimeric building blocks that sit on the surface of the lipoprotein particle. It is not clear at this
227 stage to which extent protein-lipid or protein-protein interactions prevail but both are likely
228 to be important. Indeed, NS1 dimers are known to have the ability to bind lipid membranes
229 and liposomes (7-9) and all the candidate protein ligands of NS1 published so far belong to
230 the HDL proteome (50). These proteins include complement factors C4, C1s, hnRNP C1/C2,
231 factor H, prothrombin, as well as inhibitory factors of complement clusterin, C5-9 and SC5b-
232 9 complexes (51-55). NS1 does not necessarily interact with all but it is reasonable to
233 anticipate that some will favor the association of NS1 with HDL or its stabilization. Proteomic
234 studies, direct protein-protein interaction assays, the use of synthetic HDL with defined
235 compositions or alternatively mimetic peptides will be instrumental in delineating the role of
236 the different NS1 partners in the formation of a biologically relevant NS1-HDL complex.

237
238 NS1 was previously shown to activate the immune system and impair vascular homeostasis.
239 NS1 can trigger the production of inflammatory cytokines and chemokines in cell culture and
240 in immunodeficient mice (14, 16, 56, 57). Our findings demonstrate that the formation of
241 NS1-HDL particles is a prerequisite for this effector function. The NS1-HDL complex
242 assembled *in vitro* triggers pro-inflammatory signals in primary human macrophages while
243 NS1 or HDL alone have no comparable effect. HDL particles are known to have an anti-
244 inflammatory regulatory function and contribute to the maintenance of vascular integrity
245 under physiological conditions (29, 31-33). However, it has also been reported that the
246 recruitment of specific proteins by HDL, such as serum amyloid A (SAA), confers a pro-
247 inflammatory status to these particles during an acute phase response (58-62). Our working
248 hypothesis is that NS1 exerts a similar control on HDL during dengue virus infections. This
249 process could involve the HDL scavenger receptor B1 that has recently been identified as a
250 cell surface receptor for dengue virus NS1 (Alcalà et al., BioRxiv, under review) allowing its
251 internalization in many mammalian cell types including macrophages, endothelial cells,
252 keratinocytes and hepatocytes. An NS1-HDL contribution to the cytokine storm would have
253 a direct impact on the development of severe dengue as increased levels of TNF α , IL6 and
254 IL-10 correlate consistently with disease severity and in certain instances endothelium
255 permeability (63-69).

256
257 Several studies have described altered levels of HDL, LDL or VLDL in severe dengue (70-
258 75). It is conceivable that NS1 broadly impacts the lipid and lipoprotein pathways by
259 reprogramming the signaling patterns of the different lipoprotein particles or modulating the
260 rate of their metabolic turnover. In this respect, we observed a notable change in the
261 composition of the NS1-bound lipoprotein particles with the acquisition of an ApoE-positive

262 signature over the course of the disease. ApoE is an exchangeable lipoprotein that can
263 associate with most lipoprotein particles during the lipid metabolic cycle (45, 46). ApoE has
264 also been recognized for its anti-inflammatory, anti-oxidative, anti-thrombotic and
265 endothelial repair related properties (76, 77). The changes we observe emphasize the dynamic
266 nature of the interaction of NS1 with host lipoproteins. Further studies are now needed to
267 investigate whether the formation of NS1-ApoE-positive lipoprotein complexes are part of a
268 recovery mechanism from the host or whether NS1 continues its intoxication program during
269 the convalescent phase. A number of studies have described a persistence of asthenia for
270 weeks, extending well beyond the end of the acute clinical phase (78-81).

271
272 In conclusion, we find that the secreted form of DENV protein NS1 hijacks HDL from human
273 serum, and possibly other lipoprotein particles such as LDL, to form a pro-inflammatory NS1-
274 HDL lipoprotein complex. Our data further suggest the occurrence of a structural transition
275 of NS1 on the surface of HDL that results in the collapse of NS1 hexamers and the anchoring
276 of amphipathic dimeric subunits in the HDL lipid phase. Finally, we demonstrate the presence
277 of NS1-HDL complexes in the sera of dengue patients during the acute phase of the disease.
278 The capture of HDL by NS1 may represent a way for the virus to exacerbate systemic
279 inflammation. This will affect vascular permeability and facilitate virus propagation in the
280 infected organism. Unraveling the molecular mechanisms governing the assembly of the
281 NS1-HDL complex, its metabolic fate and pathogenic functions will be critical in defining
282 preventive measures against the active form of DENV NS1.

283

284 **MATERIALS AND METHODS**

285 **DENV-2 NS1 protein expression, purification and serum pull-down experiments**

286 The DENV-2 recombinant NS1 protein was expressed in drosophila S2 cells and purified
287 from the extracellular medium as detailed in the previously published supplementary methods
288 (12). Purified DENV-2 recombinant NS1 protein was incubated for 1h at 37°C in serum or
289 plasma recovered from a healthy donor (provided by the ICAReB facility, Institut Pasteur) at
290 a final concentration of 400 µg NS1/mL plasma. The mix was then purified on a Strep-tactin
291 column (Iba), washed twice with PBS Mg²⁺/Ca²⁺ (Gibco) followed by 14 column volumes of
292 PBS 0.3 M NaCl and another 5 column volumes of PBS Mg²⁺/Ca²⁺. Elution was performed
293 using 2.5 mM D-desthobiotine (Iba) in PBS Mg²⁺/Ca²⁺.

294 Purified samples of recombinant NS1, human HDL (Millipore), human LDLs (Millipore) or
295 an *in vitro* reconstituted NS1-HDL mix were analyzed by size exclusion chromatography on
296 a Superdex 200 10/300 column (GE healthcare). Protein standards from Bio-Rad were used
297 to interpret elution profiles. The protein samples from the major peaks were further
298 denatured in 5x Laemmli sample buffer containing β-mercaptoethanol, boiled for 5 min at 95
299 °C and separated by discontinuous sodium dodecyl sulfate (SDS) 4-15% polyacrylamide gel
300 electrophoresis (SDS-PAGE precast gels, Bio-Rad). The SDS-PAGE gels were stained in
301 Coomassie Blue solution (Bio-Rad).

302

303 **Biolayer Interferometry**

304 DENV2 NS1 binding to HDL and LDL particles was monitored by Biolayer Interferometry
305 (BLI), using an Octet Red384 instrument (ForteBio). Streptavidin-coated biosensors (SA,
306 ForteBio) were loaded with biotinylated anti-ApoA-I or anti Apo-B antibodies (Abcam),

307 followed by HDL or LDL, respectively. Subsequently the biosensors were incubated in wells
308 containing serial dilutions of NS1 protein (concentrations ranging from 6.25 to 800nM for
309 HDL, and from 36 to 2500nM for LDL) and the BLI association signals were recorded in
310 real-time until they reached a plateau. Finally, the biosensors were incubated in wells
311 containing buffer to monitor the dissociation of the complexes formed, before being
312 regenerated for further use in replicate experiments. The regeneration protocol, comprising
313 three subsequent 20 seconds washes in 10 mM Gly-HCl pH2, could be applied up to eight
314 times for up to two days without losing any loading capacity of the immobilized biotinylated
315 antibodies. The specific NS1 binding curves were obtained by subtracting the non-specific
316 signals measured on unloaded biosensors used as control references. The steady-state signals
317 were determined at the end of the association step and fitted using the following equation:
318 $Req = Rmax * C / (Kd + C)$ where Req is the steady-state BLI response, C the NS1 concentration,
319 and Rmax the response at infinite concentration. All measurements were performed at least
320 three times to determine experimental errors. All experiments were performed at 20°C in PBS
321 Mg^{2+}/Ca^{2+} (Gibco) supplemented with 0.1% milk to minimize nonspecific binding, using 96-
322 well half-area plates (Greiner Bio6One) filled with 150 µl per well, and a shaking speed of
323 1000 rpm. Data was processed using the Scrubber (v2.0 BioLogic), BIAevaluation 4.0
324 (Biacore) and Profit (Quantumsoft) softwares.

325

326 **Analytical ultracentrifugation**

327 NS1, HDL, and NS1-HDL mix at different molar ratios were centrifuged at 32,000 rpm for
328 the complexes in a XL-I and a new Optima AUC (Beckman Coulter) analytical
329 ultracentrifuge, at 20 °C in a four-hole AN 50–Ti rotor equipped with 3-mm and 12-mm
330 double-sector aluminium epoxy centrepieces.

331 Detection of the biomolecule concentration as a function of radial position and time was
332 performed by absorbance measurements at 250 nm and 280 nm, and by interference detection.
333 Ultracentrifugation experiments were performed in PBS+/+ (Gibco). Sedimentation velocity
334 data analysis was performed by continuous size distribution analysis c(s) using the Sedfit 15.0
335 software (82). All the c(s) distributions were calculated with a fitted fractional ratio f/f_0 and
336 a maximum entropy regularization procedure with a confidence level of 0.95. Buffer viscosity
337 and density as well as the extinction coefficient of NS1 were calculated using the sednterp
338 software (<http://sednterp.unh.edu/>). Partial specific volume were measured for NS1 (0.82
339 ml.g⁻¹, as defined on an iodixanol density gradient) and confirmed by multidetection AUC
340 experiment for HDL (0.94 ml.g⁻¹). Extinction coefficients were extrapolated at 250 nm using
341 the Utrascan II software. Deconvolution of the multi detectors signal into stoichiometric ratio
342 was performed by integrating all the peaks on each detector to determine the contribution of
343 each partner present (NS1, HDL or both).

344

345

346 **Differential scanning calorimetry (DSC)**

347 Thermal unfolding of NS1 and of the NS1-HDL complex were followed using a VP-Capillary
348 DSC instrument (Malvern MicroCal) in PBS buffer. The concentration of the NS1 hexamer
349 was 0.2 mg/ml and was used at a 2:1 molar ratio to form the NS1-HDL complex. At least two
350 DSC scans were recorded for each sample. Human HDL (Merck Millipore) was incubated
351 with NS1 for 1 hour at 37°C prior to the DSC experiments. Scan rate was 100°C/hr with a
352 filtering period of 2. Thermograms were analysed with the Origin software provided by the
353 manufacturer.

354

355 **Electron microscopy and image analysis**

356 Solutions of NS1 and NS1-HDL were spotted on glow discharged carbon grids, contrasted
357 with 2% uranyl acetate and imaged with a Tecnai F20 microscope (Thermo Fisher, USA) in
358 low dose conditions. Automated acquisitions were performed using EPU software (Thermo
359 Fisher, USA) and images were acquired using a Falcon II (Thermo Fisher, USA) direct
360 detector.

361 HDL and NS1-HDL images were CTF-corrected (phase flip) and sorted using the XMIP
362 software (83). Corrected images were imported in Relion (84). The recommended strategy
363 for particle picking was applied as follow: a manual selection of particles compatible with the
364 HDL or NS1-HDL size was performed on a small number (about fifteen) of images. A 2D
365 classification (40 classes) was performed and five representative well-defined classes were
366 selected as template for the automatic picking, leading to about 30 000 particles. A 2D
367 classification (200 classes) was then performed. Classes obviously corresponding to artefacts
368 were suppressed and a final run of 2D classification (200 classes) was carried out.

369

370 **Macrophages immune activation assay**

371 Monocytes were isolated from buffy coats and were differentiated into macrophages by using
372 human AB serum in macrophage medium, as previously described (Allouch et al., PNAS
373 2013). Briefly, PBMCs were isolated from whole blood using a Ficol gradient centrifugation
374 (Eurobio). CD14⁺ cells are purified by magnetic bead separation of PBMCs using CD14⁺
375 human positive selection kit (StemCell) and plated 1M cells per ml on teflon plates (Sarstedt)
376 with 7 ml per plate in the following medium: RPMI-1640 (Gibco), 2 mM L-glutamine
377 (LifeTechnologies), 1% penicillin-streptomycin of concentration: 10,000 units penicillin and
378 10 mg streptomycin/ml (LifeTechnologies), 10 mM Na Pyruvate (LifeTechnologies), 10 mM

379 HEPES (LifeTechnologies), 1% MEM vitamins (LifeTechnologies), 1% NEAA
380 (LifeTechnologies), 50 uM beta-mercaptoethanol (LifeTechnologies), 15% human serum
381 (ICAREB facility, Institut Pasteur). Monocytes were cultured in differentiating media for 6-8
382 days after which the macrophages were scraped off Teflon plates and counted. After spinning,
383 they were resuspended at 1 million/ml in the same media but with 5% FBS instead of human
384 serum.

385 Macrophages were plated at 0.5 million cells per mL in P24 plates (Corning). After 2 hours
386 sedimentation and adhesion of the cells, macrophages were incubated with PBS (as negative
387 control), LPS (100 ng/mL) as positive control, HDL (2.5 µg/mL), NS1 (10 µg/mL) or a NS1-
388 HDL mix at same respective quantities (2:1 molar ratio) for 24h before collection of the
389 supernatants. Inflammatory mediators were detected in cell supernatants using a hMagnetic
390 Luminex Assay 5 Plex, R&D Systems, Bio-Techne Ltd run on the BioPlex 200 System xMAP
391 (BioRad Laboratories Inc.) as per manufacturer's specifications. The antibody bead kit was
392 designed to quantify IL-1 β , IL-6, IL-10, TNF-alpha. Standards were run with each plate at
393 every assay to titrate the level of cytokines present. Statistical analyses were performed in
394 Prism 6.0 (GraphPad Software Inc.) Data are shown as individual points and means \pm SD.
395 Significant testing was performed using 2-way ANOVA.

396

397 **DENV-infected patient sera specimen**

398 Patients presenting acute dengue-like symptoms – between June and October of 2011 and
399 2012 – were enrolled at the Kampong Cham Referral Hospital. Inclusion criteria, following
400 the WHO 1997 classification scheme, were children between 2 and 15 years old who had
401 fever or history of fever at presentation and onset of at least two of the following symptoms
402 within the previous 72 hours: headache, retro-orbital pain, muscle pain, joint pain, rash, or

403 any bleeding signs. We performed a prospective, monocentric, cross-sectional study of
404 hospitalized children with severe and non-severe dengue. The study was approved by the
405 Cambodian National Ethics Committee for Human Research (approval #087NECHR/2011).
406 All patient inclusion and blood sampling occurred after obtaining written informed consent
407 from the patient's parents or guardians. The first visit was conducted at hospital admission.
408 The day of onset of symptoms was defined as day 0 of the illness. The last visit was performed
409 at the time of discharge for patients who recovered entirely, or as a follow-up visit for patients
410 still in the critical phase. A clinical and biological follow-up including abdominal/chest
411 ultrasound recording was conducted at each visit. DENV infection of hospitalized patients
412 was confirmed by NS1 antigen detection using our NS1-capture ELISA (47-49) and/or RT-
413 qPCR and/or virus isolation on *Aedes albopictus* C6/36 cells on the plasma sample obtained
414 at admission (85). Finally, the severity of the disease among confirmed dengue patients was
415 assessed according to the WHO 2009 criteria using clinical and biological data recorded at
416 admission (ADM), follow up visit (F-VIS) or discharge (DIS).

417

418 **Capture ELISA of NS1-HDL complexes**

419 Microtitration plates were coated overnight with purified mouse anti-NS1 monoclonal
420 antibody. Wells were saturated and washed before serial dilutions of human sera spiked with
421 purified DENV-2 NS1 or DENV1- or DENV-2-infected human sera were added to wells for
422 2 h at room temperature. Wells were washed again and incubated for 1 h at 37°C with anti-
423 ApoA-I goat polyclonal antibodies followed by a peroxidase-conjugated secondary antibody
424 revealed with a 3,3', 5,5'-tetramethylbenzidine solution. Negative controls were measured
425 when the reaction was carried out in the absence of antigen. Absorbance values were corrected
426 by subtracting the mean value of the signals measured for the negative controls.

427 **FIGURE LEGENDS**

428 **Figure 1: DENV NS1 binds preferentially to human high-density lipoproteins**

429 (A) Size exclusion chromatography profile of NS1 pull-down experiments showing a clear
430 shift after incubation in complete or heat-inactivated human serum (solid and dotted black
431 lines, respectively) from the same healthy donor compared to the NS1 protein alone
432 (blue line). NS1 protein partners were identified by SDS-PAGE and N-terminal sequencing
433 as the Apolipoprotein B scaffold of the low-density lipoproteins (LDL) in the first SEC
434 elution peak, and the ApoA-I protein scaffold of the high-density lipoproteins (HDL) in the
435 second elution peak. (B) Biolayer interferometry (BLI) profiles corresponding to the binding
436 of serial-diluted concentrations of NS1 respectively to human HDL (left panel) and human
437 LDL (central panel) particles. The concentration-dependence of the steady-state signal
438 corresponding to the binding of NS1 to HDL (black dots) and LDL (white dots) is shown on
439 the right hand side panel. (C) Typical sedimentation coefficient distribution of NS1 or human
440 HDL alone or pre-incubated together (mix of NS1 and HDL at a 1:1 or 5:1 mass ratio)
441 monitored using an interferometric detector. Peaks were integrated for all the detectors
442 (interference and absorbance at 280nm). The calculated stoichiometries are indicated for each
443 peak. Solutions were equilibrated at 20°C for 2h before sedimentation velocity analysis.

444

445

446 **Figure 2: Analysis of NS1-HDL complexes by electron microscopy reveals the presence**
447 **of NS1 dimers at the surface of HDL particles**

448 (A, B) Electron microscopy observations from left to right: a representative image, followed
449 by the three most representative classes of purified HDL particles (A) and NS1-HDL
450 complexes (B). (C) Fitting of the NS1 3D structure of the dimeric form into the most abundant
451 class of NS1-HDL complexes, suggesting a collapse of the NS1 hexamer into hydrophobic
452 dimeric blocks that float and anchor into the HDL lipid phase. (D) Differential scanning
453 calorimetry (DSC) of NS1 alone (blue line) or of an NS1-HDL mix at a 2:1 molar ratio
454 (orange). Of note, the HDL particles alone did not generate any signal in the temperature
455 range tested.

456

457

458

459 **Figure 3: The NS1-HDL lipoprotein complex is biologically active in human primary**
460 **macrophages and is detectable over the clinical phase in DENV-infected patients**

461 (A) The NS1-HDL complex activates the inflammatory cytokine production from human
462 primary macrophages. After 24h incubation with respective effectors, supernatants of cell
463 culture were recovered and Luminex assays were performed to quantify the amount of TNF-
464 alpha, IL-6 and IL-10 released by cells in the extracellular medium. Data represent mean +/-
465 SEM of three independent experiments obtained using separate cells from four donors. LPS
466 stimulation was used as a positive control in the presence or absence of HDL and provided
467 values consistent between experiments. 2-Way analysis of variance (ANOVA) multiple
468 comparisons were used to assess the statistical significance of differences observed between
469 mean cytokine levels in culture supernatants between the different conditions. (B) Patients
470 (n=51) hospitalized in the Kampong Cham Referral Hospital, Cambodia, presented either
471 dengue with warning signs or severe dengue. A blood sample was recovered for each patient
472 on the day of admission at hospital and during a follow-up visit that occurred before discharge
473 from hospital (on average 4 days apart). Both samples were tested for the presence of the NS1
474 protein (upper panel), the NS1-ApoA-I complex or the NS1-ApoE complex (lower panel,
475 dark and white dots, respectively) using three different ELISA formats as described in
476 Supplementary Fig. 1. NS1-ApoA-I complexes are representative of the NS1-HDL particles
477 in plasma samples. NS1-ApoE may include different types of NS1-lipoprotein complexes as
478 ApoE is an exchangeable lipoprotein that binds to various types of lipoprotein particles at
479 different stages of their metabolic cycle.

480

481

482 **ACKNOWLEDGMENTS**

483 The authors gratefully acknowledge the staff of the Kampong Cham Referral Hospital, the
484 patients and parents who participated in the study, and the Arbovirus Team in the Virology
485 Unit at the Institut Pasteur du Cambodge who contributed to this study. We acknowledge the
486 contribution of the ICAReB facility in setting up the recruitment of donors and the acquisition
487 of blood samples, in particular Gloria Morizot, Bianca Liliana Perlaza, Sophie Chaouche,
488 Linda Sangari, Céline Chapel, Philippe Esterre and H el ene Laude. We are most grateful to
489 Christine Girard-Blanc and Evelyne Dufour for their contribution in producing and purifying
490 the recombinant DENV NS1 protein. We thank M. Nilges and the Equipex CACSICE for
491 providing the Falcon II direct detector and David Vreesler for his help in acquiring the first
492 electron microscopy images of the bovine NS1-HDL complex. Finally, we thank Alexandre
493 Pachot and Karine Kaiser for their support and helpful discussions.

494

495 **Ethics Statement**

496 The study on dengue virus-infected patients was approved by the Cambodian National Ethics
497 Committee for Human Research (approval #087NECHR/2011). All patient inclusion and
498 blood sampling occurred after obtaining written informed consent from the patient’s parents
499 or guardians.

500 Primary monocyte-derived macrophages were isolated from healthy donor blood obtained
501 from the French blood bank (Etablissement Franais du Sang) as part of a convention with
502 the Institut Pasteur. In accordance with French law, written informed consent to use the cells
503 for clinical research was obtained from each donor.

504

505

506 **FUNDING SOURCES**

507 This study benefited from the financial support of the Institut Pasteur ACIP-27-16 (to PD,
508 VD, MF); the Institut Pasteur Dengue Task Force (to MF); the Institut Pasteur INNOV-44-
509 19 (to MF); the BioMérieux collaborative program IP/BM-2012 (to MF, AS); the National
510 Natural Science Foundation of China 31600606 (to XZ); the National Key R&D Program of
511 China 2016YFA0501100 (to XZ); Guangdong Provincial Key Laboratory of Brain
512 Connectome and Behavior 2017B030301017 (to XZ); CAS Key Laboratory of Brain
513 Connectome and Manipulation 2019DP173024 (to XZ); the NIAID/NIH R01 AI24493 (E.H.)
514 and R21 AI146464 (E.H.).

515

516

517

518 **COMPETING INTERESTS**

519 Dr. Philippe Buchy is a former Head of Virology at Institut Pasteur du Cambodge and is
520 currently an employee of GSK Vaccines, Singapore.

521

522 **BIBLIOGRAPHY**

- 523 1. S. Bhatt *et al.*, The global distribution and burden of dengue. *Nature* **496**, 504 (Apr 25,
524 2013).
- 525 2. A. Wilder-Smith, E. E. Ooi, O. Horstick, B. Wills, Dengue. *Lancet* **393**, 350 (Jan 26,
526 2019).
- 527 3. S. Yacoub, J. Mongkolsapaya, G. Screaton, Recent advances in understanding dengue.
528 *F1000Res* **5**, (2016).
- 529 4. D. R. Glasner, H. Puerta-Guardo, P. R. Beatty, E. Harris, The Good, the Bad, and the
530 Shocking: The Multiple Roles of Dengue Virus Nonstructural Protein 1 in Protection and
531 Pathogenesis. *Annu Rev Virol* **5**, 227 (Sep 29, 2018).
- 532 5. M. Rastogi, N. Sharma, S. K. Singh, Flavivirus NS1: a multifaceted enigmatic viral
533 protein. *Virology journal* **13**, 131 (Jul 29, 2016).
- 534 6. D. Watterson, N. Modhiran, P. R. Young, The many faces of the flavivirus NS1 protein
535 offer a multitude of options for inhibitor design. *Antiviral research* **130**, 7 (Jun, 2016).
- 536 7. D. L. Akey, W. C. Brown, J. Jose, R. J. Kuhn, J. L. Smith, Structure-guided insights on
537 the role of NS1 in flavivirus infection. *Bioessays* **37**, 489 (May, 2015).
- 538 8. B. D. Lindenbach, C. M. Rice, *trans*-Complementation of yellow fever virus NS1 reveals
539 a role in early RNA replication. *J Virol* **71**, 9608 (1997).
- 540 9. G. Winkler, S. E. Maxwell, C. Ruebmler, V. Stollar, Newly synthesized dengue-2 virus
541 nonstructural protein NS1 is a soluble protein but becomes partially hydrophobic and
542 membrane-associated after dimerization. *Virology* **171**, 302 (Jul, 1989).
- 543 10. B. D. Lindenbach, C. M. Rice, Molecular biology of flaviviruses. *Adv Virus Res* **59**, 23
544 (2003).

- 545 11. M. Flamand *et al.*, Dengue virus type 1 nonstructural glycoprotein NS1 is secreted from
546 mammalian cells as a soluble hexamer in a glycosylation-dependent fashion. *Journal of*
547 *virology* **73**, 6104 (Jul, 1999).
- 548 12. I. Gutsche *et al.*, Secreted dengue virus nonstructural protein NS1 is an atypical barrel-
549 shaped high-density lipoprotein. *Proceedings of the National Academy of Sciences of the*
550 *United States of America* **108**, 8003 (May 10, 2011).
- 551 13. M. Flamand *et al.*, Nonstructural protein NS1 as a novel therapeutic target against
552 flaviviruses: Use of inhibiting molecules interfering with NS1 maturation or biological
553 activity. *Int. Patent* WO 2009/106986 A2 (Sept 3, 2009).
- 554 14. P. R. Beatty *et al.*, Dengue virus NS1 triggers endothelial permeability and vascular leak
555 that is prevented by NS1 vaccination. *Sci Transl Med* **7**, 304ra141 (Sep 9, 2015).
- 556 15. N. Modhiran *et al.*, Dengue virus NS1 protein activates immune cells via TLR4 but not
557 TLR2 or TLR6. *Immunol Cell Biol* **95**, 491 (May, 2017).
- 558 16. N. Modhiran *et al.*, Dengue virus NS1 protein activates cells via Toll-like receptor 4 and
559 disrupts endothelial cell monolayer integrity. *Sci Transl Med* **7**, 304ra142 (Sep 9, 2015).
- 560 17. H. Puerta-Guardo *et al.*, Flavivirus NS1 Triggers Tissue-Specific Vascular Endothelial
561 Dysfunction Reflecting Disease Tropism. *Cell Rep* **26**, 1598 (Feb 5, 2019).
- 562 18. H. Puerta-Guardo, D. R. Glasner, E. Harris, Dengue Virus NS1 Disrupts the Endothelial
563 Glycocalyx, Leading to Hyperpermeability. *PLoS pathogens* **12**, e1005738 (Jul, 2016).
- 564 19. A. C. Brault *et al.*, A Zika Vaccine Targeting NS1 Protein Protects Immunocompetent
565 Adult Mice in a Lethal Challenge Model. *Sci Rep* **7**, 14769 (Nov 7, 2017).
- 566 20. D. A. Espinosa *et al.*, Cyclic Dinucleotide-Adjuvanted Dengue Virus Nonstructural
567 Protein 1 Induces Protective Antibody and T Cell Responses. *J Immunol* **202**, 1153 (Feb
568 15, 2019).

- 569 21. J. J. Schlesinger, M. W. Brandriss, E. E. Walsh, Protection of mice against dengue 2 virus
570 encephalitis by immunization with the dengue 2 virus nonstructural glycoprotein NS1. *J*
571 *Gen Virol* **68**, 853 (1987).
- 572 22. J. J. Schlesinger, M. W. Brandriss, E. E. Walsh, Protection against 17 D yellow fever
573 encephalitis in mice by passive transfer of monoclonal antibodies to the nonstructural
574 glycoprotein gp48 and by active immunization with gp48. *J Immunol* **135**, 2805 (1985).
- 575 23. A. K. Falconar, Antibody responses are generated to immunodominant ELK/KLE-type
576 motifs on the nonstructural-1 glycoprotein during live dengue virus infections in mice
577 and humans: implications for diagnosis, pathogenesis, and vaccine design. *Clin Vaccine*
578 *Immunol* **14**, 493 (May, 2007).
- 579 24. D. Jayathilaka *et al.*, Role of NS1 antibodies in the pathogenesis of acute secondary
580 dengue infection. *Nat Commun* **9**, 5242 (Dec 7, 2018).
- 581 25. C. F. Lin, S. W. Wan, H. J. Cheng, H. Y. Lei, Y. S. Lin, Autoimmune pathogenesis in
582 dengue virus infection. *Viral Immunol* **19**, 127 (Summer, 2006).
- 583 26. S. W. Lin *et al.*, Dengue virus nonstructural protein NS1 binds to prothrombin/thrombin
584 and inhibits prothrombin activation. *J Infect*, (Nov 25, 2011).
- 585 27. D. S. Sun *et al.*, Antiplatelet autoantibodies elicited by dengue virus non-structural
586 protein 1 cause thrombocytopenia and mortality in mice. *J Thromb Haemost* **5**, 2291
587 (Nov, 2007).
- 588 28. S. W. Wan *et al.*, Anti-dengue virus nonstructural protein 1 antibodies contribute to
589 platelet phagocytosis by macrophages. *Thrombosis and Haemostasis* **115**, 646 (Mar,
590 2016).

- 591 29. R. Birner-Gruenberger, M. Schittmayer, M. Holzer, G. Marsche, Understanding high-
592 density lipoprotein function in disease: recent advances in proteomics unravel the
593 complexity of its composition and biology. *Progress in lipid research* **56**, 36 (Oct, 2014).
- 594 30. A. J. Lepedda *et al.*, Proteomic analysis of plasma-purified VLDL, LDL, and HDL
595 fractions from atherosclerotic patients undergoing carotid endarterectomy: identification
596 of serum amyloid A as a potential marker. *Oxid Med Cell Longev* **2013**, 385214 (2013).
- 597 31. L. Camont, M. J. Chapman, A. Kontush, Biological activities of HDL subpopulations
598 and their relevance to cardiovascular disease. *Trends Mol Med* **17**, 594 (Oct, 2011).
- 599 32. M. D. Saemann *et al.*, The versatility of HDL: a crucial anti-inflammatory regulator.
600 *European journal of clinical investigation* **40**, 1131 (Dec, 2010).
- 601 33. I. Ramasamy, Recent advances in physiological lipoprotein metabolism. *Clin Chem Lab*
602 *Med* **52**, 1695 (Dec, 2014).
- 603 34. K. R. Feingold, C. Grunfeld, in *Endotext*, K. R. Feingold *et al.*, Eds. (South Dartmouth
604 (MA), 2000).
- 605 35. M. E. Lauer *et al.*, Cholesteryl ester transfer between lipoproteins does not require a
606 ternary tunnel complex with CETP. *Journal of structural biology* **194**, 191 (May, 2016).
- 607 36. L. Zhang, H. Tong, M. Garewal, G. Ren, Optimized negative-staining electron
608 microscopy for lipoprotein studies. *Biochimica et biophysica acta* **1830**, 2150 (Jan,
609 2013).
- 610 37. S. Jayaraman, C. Haupt, O. Gursky, Thermal transitions in serum amyloid A in solution
611 and on the lipid: implications for structure and stability of acute-phase HDL. *Journal of*
612 *lipid research* **56**, 1531 (Aug, 2015).

- 613 38. M. Flamand, M. Chevalier, E. Henchal, M. Girard, V. Deubel, Purification and
614 renaturation of Japanese encephalitis virus nonstructural glycoprotein NS1 overproduced
615 by insect cells. *Protein Expr Purif* **6**, 519 (Aug, 1995).
- 616 39. S. Green, A. Rothman, Immunopathological mechanisms in dengue and dengue
617 hemorrhagic fever. *Curr Opin Infect Dis* **19**, 429 (Oct, 2006).
- 618 40. T. Pang, M. J. Cardoso, M. G. Guzman, Of cascades and perfect storms: the
619 immunopathogenesis of dengue haemorrhagic fever-dengue shock syndrome
620 (DHF/DSS). *Immunol Cell Biol* **85**, 43 (Jan, 2007).
- 621 41. S. Yacoub, J. Mongkolsapaya, G. Screaton, The pathogenesis of dengue. *Current opinion*
622 *in infectious diseases* **26**, 284 (Jun, 2013).
- 623 42. J. Fink, F. Gu, S. G. Vasudevan, Role of T cells, cytokines and antibody in dengue fever
624 and dengue haemorrhagic fever. *Rev Med Virol* **16**, 263 (Jul-Aug, 2006).
- 625 43. S. Alcon *et al.*, Enzyme-linked immunosorbent assay specific to Dengue virus type 1
626 nonstructural protein NS1 reveals circulation of the antigen in the blood during the acute
627 phase of disease in patients experiencing primary or secondary infections. *Journal of*
628 *Clinical Microbiology* **40**, 376 (Feb, 2002).
- 629 44. P. Dussart *et al.*, Evaluation of an enzyme immunoassay for detection of dengue virus
630 NS1 antigen in human serum. *Clinical and vaccine immunology : CVI* **13**, 1185 (Nov,
631 2006).
- 632 45. A. D. Marais, Apolipoprotein E in lipoprotein metabolism, health and cardiovascular
633 disease. *Pathology* **51**, 165 (Feb, 2019).
- 634 46. X. Su, D. Peng, The exchangeable apolipoproteins in lipid metabolism and obesity. *Clin*
635 *Chim Acta* **503**, 128 (Apr, 2020).

- 636 47. S. Alcon-LePoder *et al.*, Secretion of flaviviral non-structural protein NS1: from
637 diagnosis to pathogenesis. *Novartis Foundation symposium* **277**, 233 (2006).
- 638 48. P. Antunes *et al.*, Quantification of NS1 dengue biomarker in serum via optomagnetic
639 nanocluster detection. *Sci Rep* **5**, 16145 (Nov 5, 2015).
- 640 49. D. H. Libraty *et al.*, High circulating levels of the dengue virus nonstructural protein NS1
641 early in dengue illness correlate with the development of dengue hemorrhagic fever. *J*
642 *Infect Dis* **186**, 1165 (2002).
- 643 50. B. Shao, J. W. Heinecke, Quantifying HDL proteins by mass spectrometry: how many
644 proteins are there and what are their functions? *Expert Rev Proteomics* **15**, 31 (Jan, 2018).
- 645 51. P. Avirutnan *et al.*, Vascular leakage in severe dengue virus infections: a potential role
646 for the nonstructural viral protein NS1 and complement. *J Infect Dis* **193**, 1078 (Apr 15,
647 2006).
- 648 52. W. E. Brandt, R. D. Cardiff, P. K. Russell, Dengue virions and antigens in brain and
649 serum of infected mice. *J. Virol.* **6**, 500 (1970).
- 650 53. K. M. Chung *et al.*, West Nile virus nonstructural protein NS1 inhibits complement
651 activation by binding the regulatory protein factor H. *Proc Natl Acad Sci U S A* **103**,
652 19111 (Dec 12, 2006).
- 653 54. T. Kurosu, P. Chaichana, M. Yamate, S. Anantapreecha, K. Ikuta, Secreted complement
654 regulatory protein clusterin interacts with dengue virus nonstructural protein 1. *Biochem*
655 *Biophys Res Commun* **362**, 1051 (Nov 3, 2007).
- 656 55. J. N. Conde *et al.*, Inhibition of the Membrane Attack Complex by Dengue Virus NS1
657 through Interaction with Vitronectin and Terminal Complement Proteins. *Journal of*
658 *virology* **90**, 9570 (Nov 1, 2016).

- 659 56. F. Alayli, F. Scholle, Dengue virus NS1 enhances viral replication and pro-inflammatory
660 cytokine production in human dendritic cells. *Virology* **496**, 227 (Sep, 2016).
- 661 57. J. Chen, M. M. Ng, J. J. Chu, Activation of TLR2 and TLR6 by Dengue NS1 Protein and
662 Its Implications in the Immunopathogenesis of Dengue Virus Infection. *PLoS pathogens*
663 **11**, e1005053 (Jul, 2015).
- 664 58. G. Marsche, M. D. Saemann, A. Heinemann, M. Holzer, Inflammation alters HDL
665 composition and function: implications for HDL-raising therapies. *Pharmacology &*
666 *therapeutics* **137**, 341 (Mar, 2013).
- 667 59. O. Murch, M. Collin, C. J. Hinds, C. Thiemermann, Lipoproteins in inflammation and
668 sepsis. I. Basic science. *Intensive Care Med* **33**, 13 (Jan, 2007).
- 669 60. C. Kopecky, G. Michlits, M. D. Saemann, T. Weichhart, Pro- versus Anti-inflammatory
670 Actions of HDLs in Innate Immunity. *Cell Metab* **26**, 2 (Jul 5, 2017).
- 671 61. N. Prufer, B. Kleuser, M. van der Giet, The role of serum amyloid A and sphingosine-1-
672 phosphate on high-density lipoprotein functionality. *Biological chemistry* **396**, 573 (Jun,
673 2015).
- 674 62. A. Wu, C. J. Hinds, C. Thiemermann, High-density lipoproteins in sepsis and septic
675 shock: metabolism, actions, and therapeutic applications. *Shock* **21**, 210 (Mar, 2004).
- 676 63. B. E. Dewi, T. Takasaki, I. Kurane, In vitro assessment of human endothelial cell
677 permeability: effects of inflammatory cytokines and dengue virus infection. *Journal of*
678 *virological methods* **121**, 171 (Nov, 2004).
- 679 64. J. Huang *et al.*, Serum Cytokine Profiles in Patients with Dengue Fever at the Acute
680 Infection Phase. *Dis Markers* **2018**, 8403937 (2018).

- 681 65. Y. H. Lee, W. Y. Leong, A. Wilder-Smith, Markers of dengue severity: a systematic
682 review of cytokines and chemokines. *The Journal of general virology* **97**, 3103 (Dec,
683 2016).
- 684 66. A. Rathakrishnan *et al.*, Cytokine expression profile of dengue patients at different phases
685 of illness. *PLoS One* **7**, e52215 (2012).
- 686 67. F. Tramontini Gomes de Sousa Cardozo *et al.*, Serum from dengue virus-infected patients
687 with and without plasma leakage differentially affects endothelial cells barrier function
688 in vitro. *PLoS One* **12**, e0178820 (2017).
- 689 68. K. S. Abhishek *et al.*, Association of interleukin-2, -4 and -10 with dengue severity.
690 *Indian J Pathol Microbiol* **60**, 66 (Jan-Mar, 2017).
- 691 69. A. Srikiatkachorn, A. Mathew, A. L. Rothman, Immune-mediated cytokine storm and
692 its role in severe dengue. *Semin Immunopathol* **39**, 563 (Jul, 2017).
- 693 70. E. C. van Gorp *et al.*, Changes in the plasma lipid profile as a potential predictor of
694 clinical outcome in dengue hemorrhagic fever. *Clin Infect Dis* **34**, 1150 (Apr 15, 2002).
- 695 71. E. Barrientos-Arenas *et al.*, [Modulation of high-density lipoprotein and cytokine IL-
696 1beta and IL-6 levels in patients with dengue]. *Rev Peru Med Exp Salud Publica* **35**, 15
697 (Jan-Mar, 2018).
- 698 72. J. C. Suvarna, P. P. Rane, Serum lipid profile: a predictor of clinical outcome in dengue
699 infection. *Trop Med Int Health* **14**, 576 (Feb 27, 2009).
- 700 73. H. H. Biswas *et al.*, Lower Low-Density Lipoprotein Cholesterol Levels Are Associated
701 with Severe Dengue Outcome. *PLoS neglected tropical diseases* **9**, e0003904 (2015).
- 702 74. D. Marin-Palma, C. M. Sirois, S. Urcuqui-Inchima, J. C. Hernandez, Inflammatory status
703 and severity of disease in dengue patients are associated with lipoprotein alterations.
704 *PLoS One* **14**, e0214245 (2019).

- 705 75. W. G. Lima, N. A. Souza, S. O. A. Fernandes, V. N. Cardoso, I. P. Godoi, Serum lipid
706 profile as a predictor of dengue severity: A systematic review and meta-analysis. *Reviews*
707 *in medical virology* **29**, e2056 (Sep, 2019).
- 708 76. S. Filou *et al.*, Distinct Roles of Apolipoproteins A1 and E in the Modulation of High-
709 Density Lipoprotein Composition and Function. *Biochemistry* **55**, 3752 (Jul 12, 2016).
- 710 77. E. K. Valanti, K. Dalakoura-Karagkouni, D. Sanoudou, Current and Emerging
711 Reconstituted HDL-apoA-I and HDL-apoE Approaches to Treat Atherosclerosis. *J Pers*
712 *Med* **8**, (Oct 3, 2018).
- 713 78. D. C. Tiga-Loza *et al.*, Persistence of symptoms in dengue patients: a clinical cohort
714 study. *Transactions of the Royal Society of Tropical Medicine and Hygiene*, (Mar 3,
715 2020).
- 716 79. L. A. S. Teixeira, F. Nogueira, G. A. N. Nascentes, Prospective study of patients with
717 persistent symptoms of dengue in Brazil. *Rev Inst Med Trop Sao Paulo* **59**, e65 (Sep 4,
718 2017).
- 719 80. L. L. Luengas, D. C. Tiga, V. M. Herrera, L. A. Villar-Centeno, Characterization of the
720 health condition of people convalescing from a dengue episode. *Biomedica* **36**, 89 (Dec
721 7, 2015).
- 722 81. E. S. Halsey *et al.*, Occurrence and correlates of symptom persistence following acute
723 dengue fever in Peru. *The American journal of tropical medicine and hygiene* **90**, 449
724 (Mar, 2014).
- 725 82. P. H. Brown, P. Schuck, Macromolecular size-and-shape distributions by sedimentation
726 velocity analytical ultracentrifugation. *Biophysical journal* **90**, 4651 (Jun 15, 2006).

- 727 83. J. A. Velazquez-Muriel, C. O. Sorzano, S. H. Scheres, J. M. Carazo, SPI-EM: towards a
728 tool for predicting CATH superfamilies in 3D-EM maps. *J Mol Biol* **345**, 759 (Jan 28,
729 2005).
- 730 84. S. H. Scheres, RELION: implementation of a Bayesian approach to cryo-EM structure
731 determination. *Journal of structural biology* **180**, 519 (Dec, 2012).
- 732 85. A. C. Andries *et al.*, Value of Routine Dengue Diagnostic Tests in Urine and Saliva
733 Specimens. *PLoS neglected tropical diseases* **9**, e0004100 (Sep, 2015).
- 734
- 735
- 736

Fig. 1

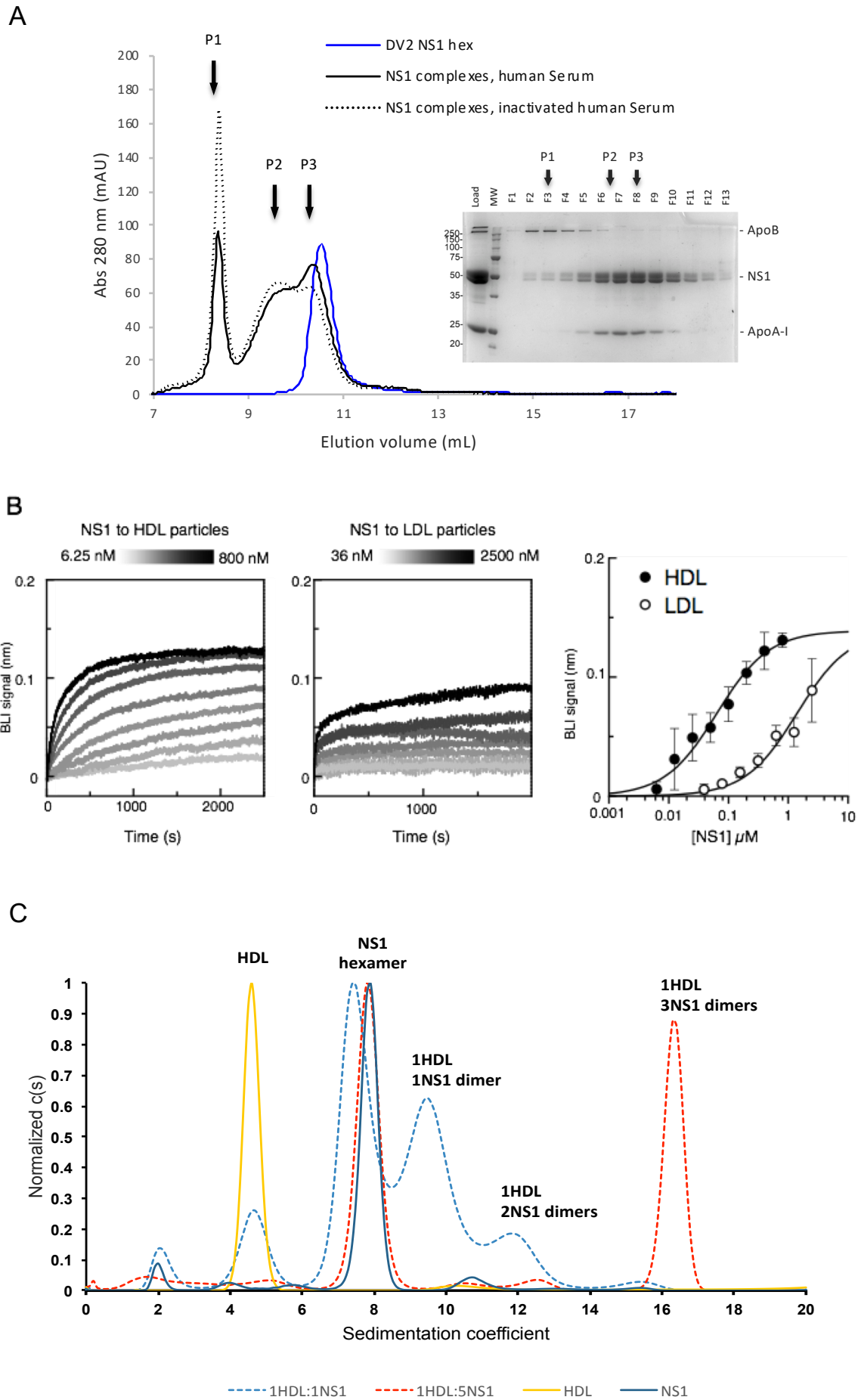


Fig. 2

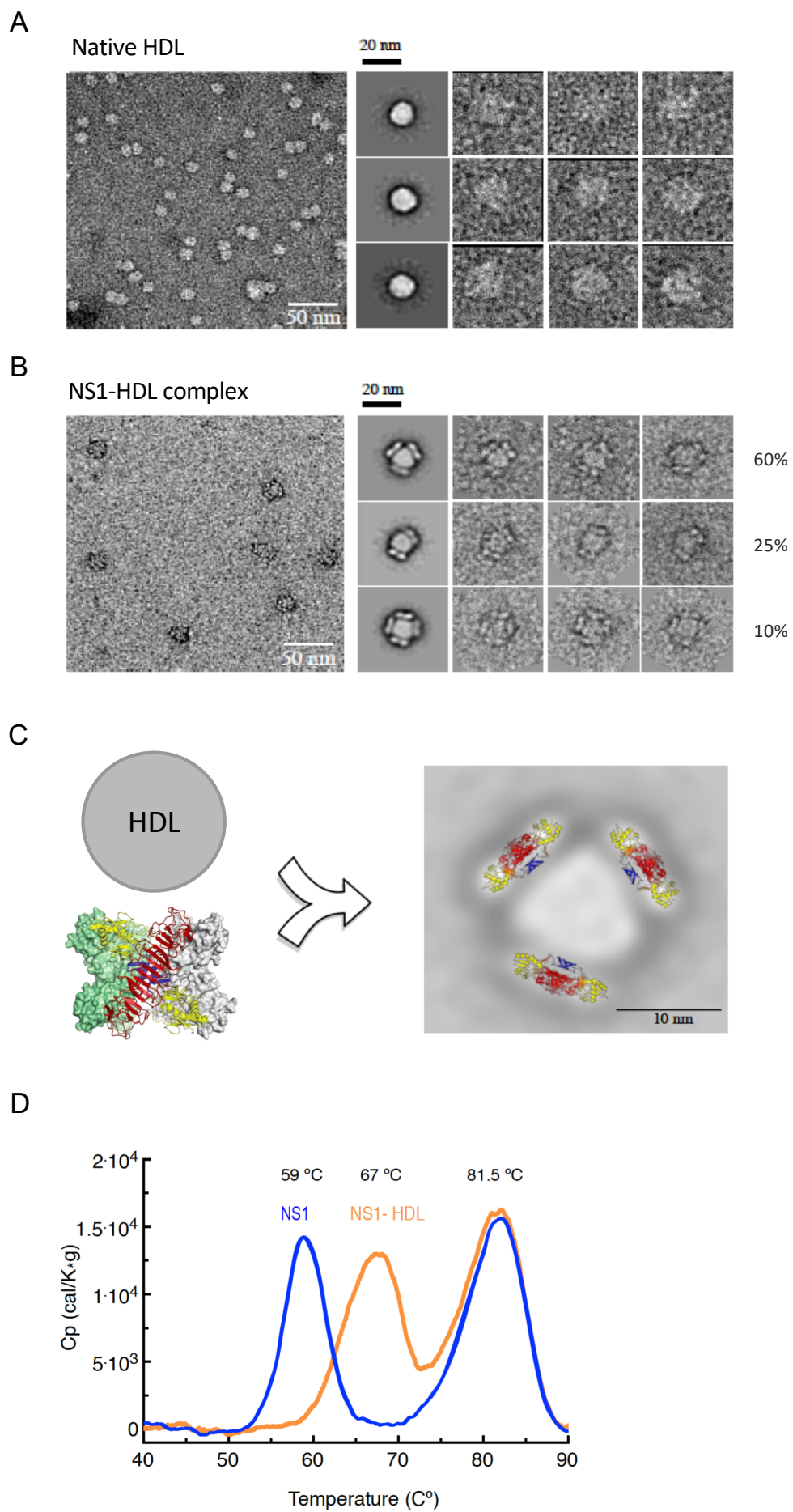
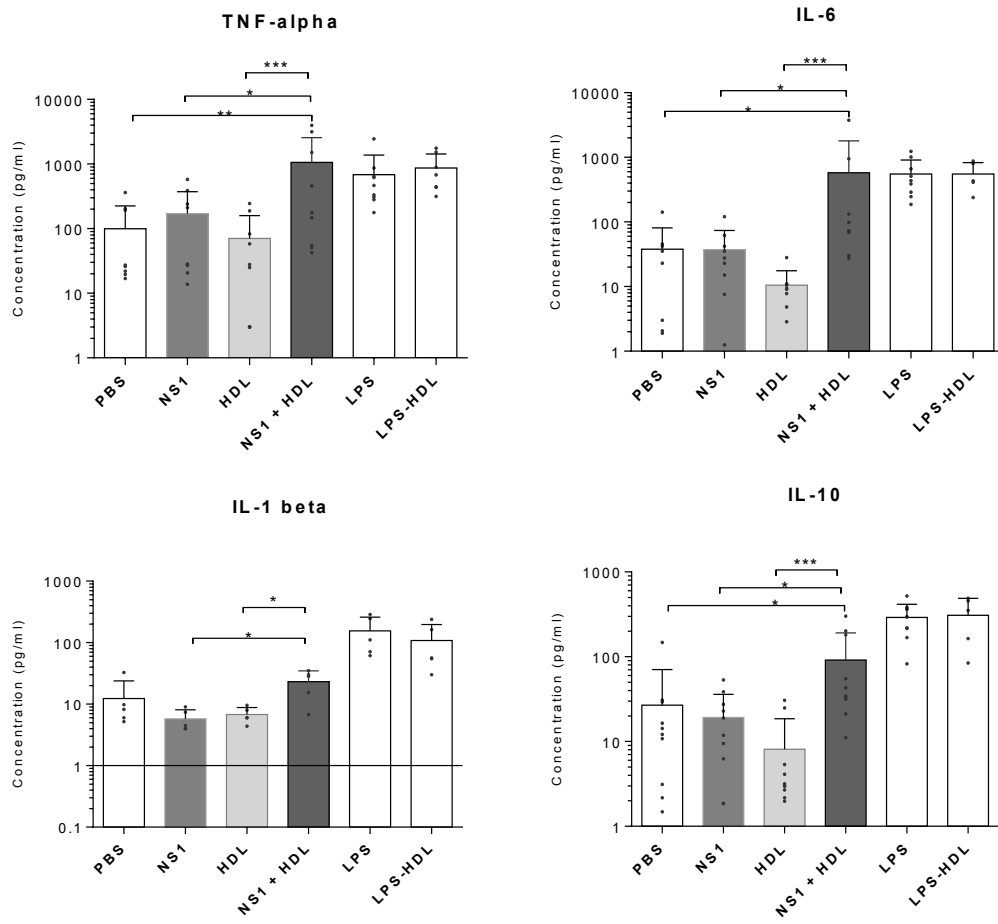


Fig. 3

A



B

